

Seismicity of the Algerian Tell Atlas and the Impacts of Major Earthquakes



Farida Ousadou and Mourad Bezzeghoud

Abstract The seismicity of the Tell Atlas, which extends from the Algerian margin to the South Atlantic fault system, is related to the dynamics of Quaternary basins under an oblique NW–SE convergent stress regime, including the basins of Mleta and L’Habra in the west, Cheliff and Mitidja in the centre, and Soummam, Hodna and Guelma in the east. This seismicity is characterized by moderate to low magnitudes with strong events occurring generally once a decade. Over the last six decades, several moderate, strong and major events occurred that were associated with extensive and severe damage, such as those of El Asnam (1954, M_s 6.7; 1980, M_s 7.3), Constantine (1985, M_s 6.0), Tipasa–Chenoua (1989, M_s 6.0), Mascara (1994, M_s 6.0), Ain Temouchent (1999, M_s 5.8), Beni Ouartilane (2001, M_s 5.6), Zemmouri—Boumerdes (2003, M_w 6.8) and Laalam (2005, M_s 5.8), in addition to numerous large historical seismic events, including those that occurred in Algiers (1365 and 1716, $I_o = X$), Oran (1790, $I_o = X$), Mascara (1819, $I_o = X$), Djidjelli (1856, $I_o = VIII$) and M’sila (1885, $I_o = IX$). This chapter presents a review of the seismicity of North Algeria and a detailed analysis of the main earthquakes that have occurred in the Tell Atlas since 1980. Finally, the impacts of several significant earthquakes that occurred during the period between 1364 and 2015 are presented and discussed in terms of seismic energy.

Keywords Seismicity · Focal mechanisms · Seismic energy
Impact of earthquakes · North Algeria

F. Ousadou

Centre de Recherche en Astronomie, Astrophysique et Géophysique, BP 63,
16340 Bouzaréah, Algiers, Algeria

M. Bezzeghoud (✉)

Departamento de Física, Escola de Ciências e Tecnologia (ECT), Instituto de Ciências da Terra (IIFA), University of Évora, Colégio Luis Antonio Verney, Romão Ramalho, 59,
7002-554 Évora, Portugal
e-mail: mourad@uevora.pt

© Springer Nature Switzerland AG 2019

A. Bendaoud et al. (eds.), *The Geology of the Arab World—An Overview*,
Springer Geology, https://doi.org/10.1007/978-3-319-96794-3_11

401

1 Introduction

The western part of the Eurasia–Nubia plate boundary extends from the Mid-Atlantic Ridge in the west to Tunisia in the east, and includes the Iberian Peninsula and the northern part of the Maghreb region. The interaction between Iberia and Nubia results in a complex region located in the western part of the Eurasian–African plate boundary that has various tectonic features (Buform et al. 2004; Borges et al. 2007, 2008; Bezzeghoud et al. 2014). This region corresponds to the transition from an oceanic boundary (between the Azores islands and the Gorringe Bank) to a continental boundary where Iberia and Nubia collide.

According to several authors, (Buform et al. 2004; Borges et al. 2007; Bezzeghoud et al. 2014), in the Ibero-Maghrebian region between the Gulf of Cadiz and Algeria, the Eurasian–Nubian plate boundary corresponds to a well-defined narrow band of seismicity, where large earthquakes occur in association with N–S to NNW–SSE horizontal compression due to the convergence of Eurasia and Nubia (Fig. 1). In this region, earthquakes are concentrated between 2°W and 4°E, and $M > 6.0$ earthquakes have occurred on 9 September 1954 (M_s 6.5, El Asnam, formerly Orléansville, Algeria); 10 October 1980 (M_s 7.3, El Asnam, formerly Chlef, Algeria); 27 October 1985 (M_w 5.9, Constantine, Algeria); 29 October 1989 (M_w 6.0 Tipasa–Chenoua, Algeria); 18 August 1994 (M_w 5.7, Mascara, Algeria); 22 December 1999 (M_w 5.7, Ain Temouchent, Algeria); 10 November 2000 (M_s 5.5, Beni Ouartilane, Algeria); 21 May 2003 (M_w 6.8, Zemmouri–Boumerdes, Algeria) (Ayadi and Bezzeghoud 2015); 24 February 2004 (M_w 6.4, Al Hoceima, Morocco) (Buform et al. 2004); 20 March 2006, (M_w 5.2, Laalam, Algeria) (Bouhadad et al. 2010) and 2016 south Alboran earthquake (M_w 6.4) (Buform et al. 2017).

Intermediate-depth seismicity (60–150 km) in the Alboran Sea region extends, in the N–S direction, in a very narrow vertical band of 50 km wide. This intermediate-depth seismicity is distributed in E–W direction and limited by a narrow band less than 20 km wide that broadens as we move to the Strait of Gibraltar. This seismicity could also be associated with the convergence process of the Eurasia–Africa plates (Buform et al. 2004). This intermediate-depth seismic activity on the eastern side of the Strait of Gibraltar may be explained by the existence of a seismogenic block in the upper mantle that has approximate dimensions of 200 km long, 150 km deep and 50 km wide (Buform et al. 2004). In this region, the material is relatively rigid, and the stresses are released by larger earthquakes. The presence of very deep earthquakes (650 km) under southern Spain is a further sign of the complexity of this area. In the Alboran Sea region, the material is more fragmented with a large number of small faults, and the stresses are released by frequent small-to-moderate earthquakes. Consequently, the plate boundary is more diffuse and corresponds to a wider area that includes the Betics, the Alboran Sea and the Rif Cordilleras (Buform et al. 2004), where deformation is manifested by the continuous occurrence of small earthquakes and only occasionally by moderate to strong earthquakes with magnitudes greater than six as shown by the historical seismicity (Martínez Solares and Mezcuá 2002; El Mrabet

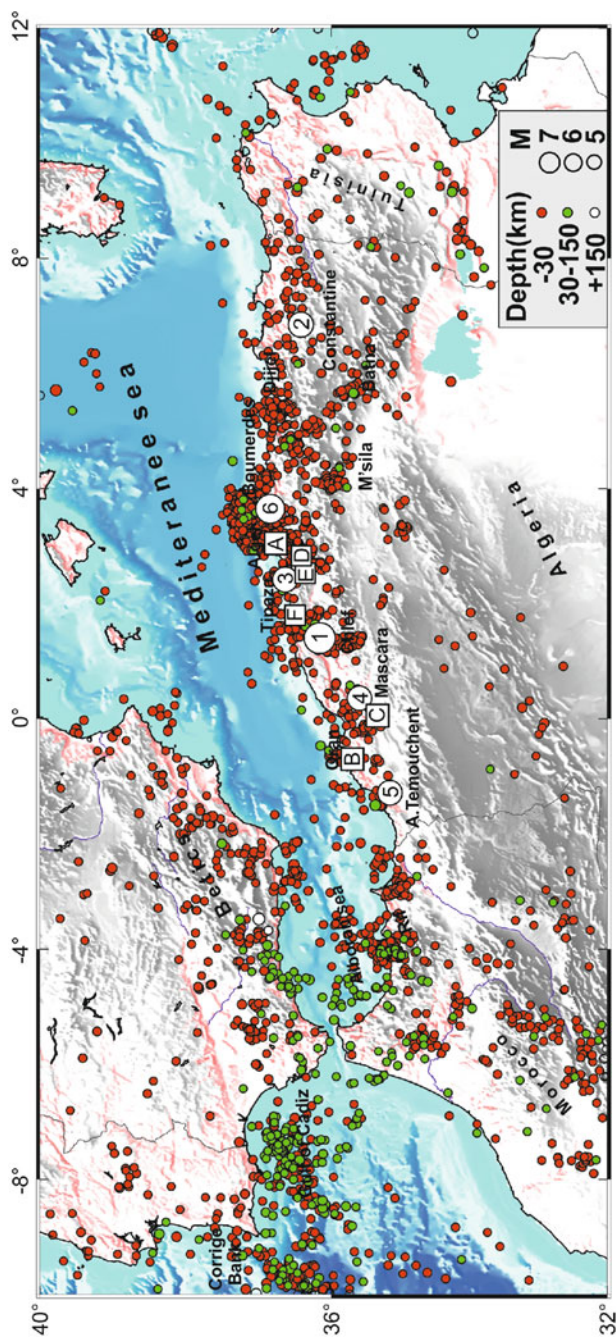


Fig. 1 Seismicity ($M \geq 4.5$) of the Ibero-Maghrebian region for 1973–2015. Seismic data were taken from the NEIC database. White squares are the major historical earthquakes (A: 02/01/1365, B: 09/10/1790, C: -03/1819, D: 02/03/1825, E: 02/01/1867, F: 15/01/1891). White circles are the main earthquakes discussed in this study (1: 1980 El Asnam EQ, 2: 1985 Constantine EQ, 3: 1989 Tipaza Chenoua EQ). The topography and bathymetry data have been extracted from the GEBCO (General Bathymetric Chart of the Oceans: <http://www.gebco.net>). Figures 1, 2, 3, 4, 5 and 6 are plotted with GMT software (Wessel and Smith 1991)

2005; Bahrouni et al. 2013; Ayadi and Bezzeghoud 2015). This intermediate and deep seismicity recorded beneath the Gibraltar Arc, the westernmost Alboran Sea and southern Spain remains a subject of debate concerning whether it may be attributed to active subduction beneath the Gibraltar Arc or to another origin (Gutscher et al. 2012).

The stress regime obtained from the focal mechanisms of shallow events is compatible with the horizontal N–S to NW–SE convergence of Eurasia and Africa. However, in the Betics–Alboran area, there is also horizontal extension in an approximately E–W direction (De Vicente et al. 2008; Van der Woerd et al. 2014). According to several authors (e.g. Houseman 1996; Buforn et al. 2004) different tectonic models have been proposed for this region such as subduction process, extensional collapse of thickened continental lithosphere, continental lithospheric delamination, back-arc extension caused by subduction rollback, convective thinning, or subduction and breaking of a vertical slab of material.

Thus, for the Central Maghreb, the stress regime obtained from the inversion of focal mechanisms reflects a ‘pure’ convergence dynamic in the NW–SE direction and for both sides (the Rif in northern Morocco and northern Tunisia) reflects a strike–slip regime. Both sides are affected by the geodynamics of the adjacent areas that are influenced by the dynamics of the Alboran Sea in northwestern Morocco (Ousadou et al. 2014) and by lateral slab migration/segmentation and deep dynamics such as lithosphere–mantle interactions in the Tunisian Atlas (Soumaya et al. 2015).

The convergence rate determined by seismic strain analysis decreases from the Azores Plateau to the Ibero-Maghrebian region (Bezzeghoud et al. 2008, 2014; Buforn 2008). The corresponding values of slip velocity given by Bezzeghoud et al. (2014) range between 1.4 and 6.7 mm/year from the triple junction to the northwestern part of Algeria and the Tell Mountains, where the velocity is approximately 3.7 mm/year. These values may underestimate the geological deformation and do not include the energy released by aseismic processes (e.g. folding, thickening, plastic deformation and slow aseismic slip). Additionally, the slip velocity may be considered to be instantaneous and independent from that derived from the geodetic data because the earthquake cycle is much shorter than the history of available earthquakes (Borges et al. 2007).

2 Seismicity of Algeria in the Ibero-Maghrebian Context

2.1 *Seismicity of the Ibero-Maghrebian Region*

The seismicity of the Maghreb region is located along the African–Eurasian plate boundary starting from the Azores triple junction and continuing to Tunisia, crossing the Strait of Gibraltar, Morocco and northern Algeria. It is related to the closure of Quaternary basins under an oblique NW–SE convergent stress regime.

Most of the activity is linked to fault-related folds striking NE–SW and is distributed along the main tectonic features. Because the plate boundary is not defined by a single discontinuity, as found in the western region of Gibraltar, but is more diffuse, the earthquakes are distributed over a wide zone. Most of the seismicity is shallow, located between depths of 5 and 20 km (Fig. 1). Nevertheless, intermediate and deep seismic events have been observed beneath the Gibraltar Arc, the westernmost Alboran Sea and southern Spain. The seismicity distribution in the Maghreb displays a clear arrangement for the activity since 1973, with an E–W trend along the African–Eurasian plate boundary (Fig. 1). Morocco and Algeria appear as more active areas than Tunisia, and the seismicity is mainly concentrated in the Rif, the High Atlas of Morocco, the Algerian Tell and Middle Atlas and the Tunisian Atlas, where the seismicity spreads along a band extending south to the Saharan Atlas (Fig. 1). The easternmost Maghrebian region, the Tunisian Atlas area, has not experienced strong earthquakes; most of the seismicity is of low magnitude located in the Northwestern Atlas, Southern Atlas and Eastern Pelagic platform (Bahrouni et al. 2013, 2014). However, Tunisia is still a key region because it is located at the junction between the eastern and western Mediterranean domains and straddles the orogenic province and the stable platform (Bouaziz et al. 2002).

In the Ibero-Maghrebian region, the NW–SE oblique convergence between Africa and Eurasia plates is consistent with the earthquake focal mechanisms that show mostly reverse faulting on NE–SW trending often combined with a strike–slip component. Most of the focal mechanisms in this area exhibit strike–slip faulting in northern Morocco, reverse faulting in northwestern Algeria and strike–slip mechanisms in northeastern Algeria and Tunisia (Fig. 2) (Ayadi et al. 2002; Bezzeghoud and Buforn 1999; Harbi et al. 1999; Buforn et al. 2004; Bahrouni et al. 2014). This agrees with earlier studies that give a NW–SE convergence direction for Africa and Eurasia with translation of the African plate to the east.

2.2 *Seismicity of Algeria*

The seismicity of the Tell Atlas, which extends from the Algerian margin to the South Atlasic fault system, is related to the dynamics of Quaternary basins under an oblique NW–SE convergent stress regime, including the basins of Mleta and L’Habra in the west, Chelif and Mitidja in the centre, and Soummam, Hodna and Guelma in the east. Most of the activity is linked to fault-related folds striking NE–SW and is distributed along the main tectonic features. This seismicity is characterized by moderate to low magnitude with strong events occurring generally once a decade. Over the last six decades, several strong events occurred and were associated with extensive and severe damage. The seismic catalogues show several moderate, strong and major events offshore or inland, such as those listed in the introduction in addition to numerous large historical events such as those that occurred in Algiers (1365 and 1716, $I_0 = X$), Oran (1790, $I_0 = X$), Mascara (1819,

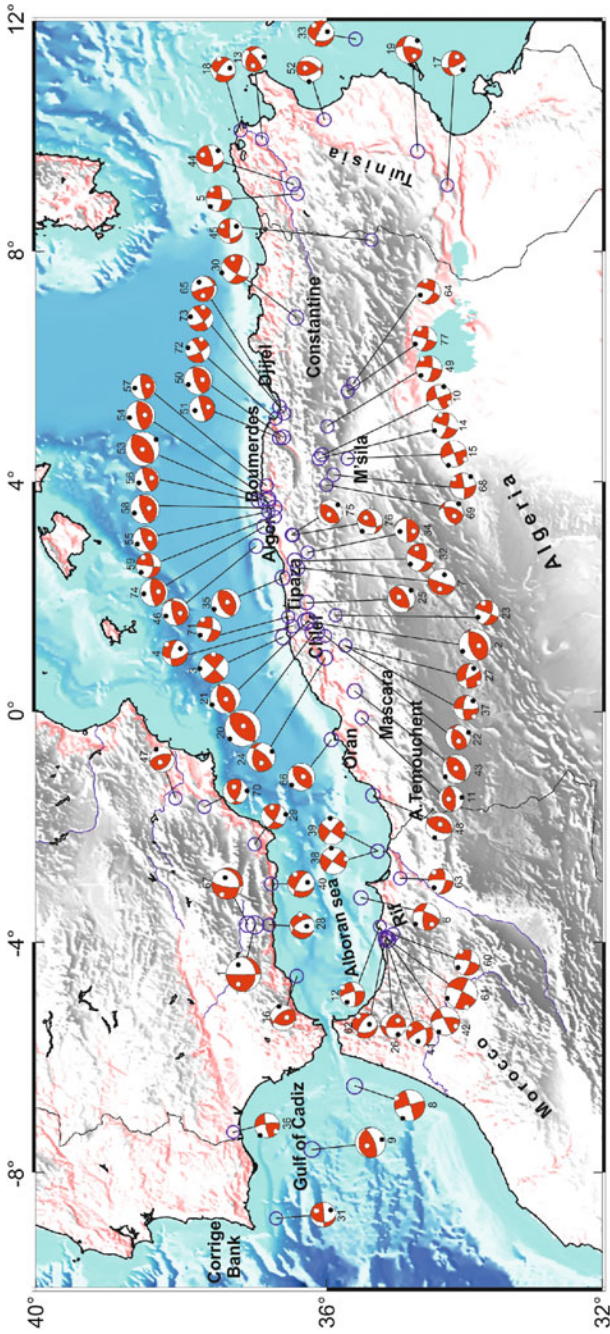


Fig. 2 Focal mechanisms for $M \geq 5.0$ shallow earthquakes (depth ≤ 40 km) in the Ibero-Maghrebian region for the period 1950–2015. Size is proportional to magnitude. Solution parameters for focal mechanisms are listed in Table 2

$I_0 = X$), Djidjelli (1856, $I_0 = VIII$) and M'sila (1885, $I_0 = IX$) (Benouar 1994; Mokrane et al. 1994; Harbi et al. 2010; 2015; Ayadi and Bezzeghoud 2015).

The focal mechanisms in Algeria are dominated by reverse faulting for earthquakes located in the western part of the country from 2°W to 5°E, which are associated with the strong and moderate earthquakes that occurred in the area (Fig. 2). Meanwhile, the focal mechanisms in the eastern part are dominated by strike-slip faulting for earthquakes located from 5°E to 8°E (Fig. 2). Most of these are associated with identified active Quaternary faults and folds (Bouhadad et al. 2003; Ayadi et al. 2002, 2008; Meghraoui 1988; Bounif et al. 1987; Maouche et al. 2011; Abbes et al. 2016).

3 Significant Earthquakes in Algeria Since 1980

Among all the earthquakes that have occurred in Algeria, we present only those with magnitudes greater than or equal to 5.7 and caused serious damage (Table 1) for the period 1980–2016. These earthquakes include the following: (i) the El Asnam earthquake of 10 October 1980, with M_w 7.1; (ii) the Constantine earthquake of 27 October 1985, with M_w 5.9; (iii) the Tipasa–Chenoua earthquake of 29 October 1989, with M_w 6.0; (iv) the Mascara earthquake of 22 August 1994, with M_w 5.7; (v) the Ain Temouchent earthquake of 22 December 1999, with M_w 5.7 and (vi) the Zemmouri—Boumerdes earthquake of 21 May 2003, with M_w 6.8.

3.1 The El Asnam Earthquake of 10 October 1980

The strongest event that occurred in northern Africa is that of El Asnam on 10 October 1980, at 12 h 25 min (TU) with M_s 7.3 (Table 1). This event has been

Table 1 Damage caused by the most significant earthquakes occurred in Algeria since 1980 discussed in the text. The damage is given by Mr. Chergui Abdelkader and Mrs. Bradai Kheira from the 'Direction Générale de la Protection Civile' (Algiers, Algeria)

Date	Location	M_w	Damage
10/10/1980	El Asnam (now known as Chlef)	7.1	2633 killed, 8369 injured and 30,022,000 inhabitants homeless
27/10/1985	Constantine	5.9	10 killed and 300 injured
29/10/1989	Tipasa–Chenoua	6.0	22 killed, 250 injured and 50,000 inhabitants homeless
18/08/1994	Mascara	5.7	171 killed, 270 injured and 10,000 inhabitants homeless
22/12/1999	Ain Témouchent	5.7	28 killed, 174 injured and 25,000 inhabitants homeless
21/05/2003	Zemmouri—Boumerdes	6.8	2278 killed and 11,452 injured

Table 2 Source parameters of focal mechanisms plotted in Fig. 2

Date	LAT	LON	Depth	Strike	DIP	Rate	M	n°	References
20/03/1954	37	-3.7	640	179	88	-122	7.0	1	Bufoim et al. (1991)
09/09/1954	36.28	1.57	7	253	61	104	6.5	2	Espinoza and Lopez (1984)
10/09/1954	36.6	1.3	8	44	90	-8	6.0	3	Dewey (1990)
05/06/1955	36.4	1.6	13	172	56	-32	5.2	4	Shirokova (1967)
20/02/1957	36.4	9	10	185	87	18	5.2	5	Hfaiedh et al. (1985), Soumaya et al. (2015)
23/08/1959	35.51	-3.23	20	276	70	153	5.5	6	Bezzeghoud and Bufoim (1999)
07/11/1959	36.4	2.5	7	203	10	-5	5.6	7	Henares et al. (2003)
05/12/1960	35.6	-6.5	15	73	86	-178	6.2	8	Bufoim et al. (2004)
15/03/1964	36.2	-7.6	12	276	24	117	6.1	9	Bufoim et al. (2004)
01/01/1965	35.7	4.4	13	340	90	12	5.1	10	Hatzfeld (1978)
13/07/1967	35.5	-0.1	5	260	30	87	5.1	11	Bufoim et al. (2004)
17/04/1968	35.24	-3.73	22	83	70	-162	5.0	12	Bufoim et al. (2004)
01/12/1970	36.9	9.95	15	49	74	50	5.1	13	Hfaiedh et al. (1985), Soumaya et al. (2015)
24/11/1973	36.1	4.4	15	200	89.9	14	5.2	14	Hatzfeld (1978)
24/11/1973	36.06	4.47	8	70	86	-176	5.3	15	Hatzfeld (1978)
07/08/1975	36.41	-4.59	28	186	42	138	5.2	16	Henares et al. (2003)
08/02/1978	34.27	9.15	30	266	54	26	5.0	17	Mezcua and Martinez Solares (1983)
09/04/1979	37.2	10.1	12	305	67	-140	5.0	18	Gueddiche et al. (1992), Soumaya et al. (2015)
08/12/1979	34.7	9.74	33	7	72	35	5.4	19	Ben Ayed and Zargouni (1990)
10/10/1980	36.16	1.39	12	225	54	83	7.3	20	Ouyed et al. (1981)
10/10/1980	36.24	1.59	10	58	43	81	6.1	21	Harvard CMT
08/11/1980	36.02	1.32	5	270	45	126	5.0	22	Bezzeghoud et al. (2012)
05/12/1980	35.87	1.68	5	112	61	-179	5.0	23	Bezzeghoud et al. (2012)
07/12/1980	36.02	0.94	5	277	40	140	5.8	24	Bezzeghoud and Bufoim (1999)

(continued)

Table 2 (continued)

Date	LAT	LON	Depth	Strike	DIP	Rake	M	n°	References
01/02/1981	36.27	1.9	11	210	43	64	5.5	25	Bezzeghoud and Buform (1999)
07/04/1981	35.12	-3.98	4	182	75	132	5.0	26	Bezzeghoud et al. (2012, 2014)
15/11/1982	35.73	1.15	7	274	70	-169	5.0	27	Bezzeghoud et al. (2012, 2014)
24/06/1984	36.8	-3.7	5	201	48	-46	5.0	28	Bezzeghoud and Buform (1999)
13/09/1984	37	-2.3	9	121	73	156	5.1	29	Buform et al. (2004)
27/10/1985	36.42	6.85	10	213	71	20	5.9	30	Harvard CMT
20/10/1986	36.7	-8.8	37	180	37	3	5.0	31	Bezzeghoud et al. (2012, 2014)
31/10/1988	36.44	2.63	13	103	55	167	5.7	32	Bezzeghoud and Buform (1999)
06/01/1989	35.59	11.69	11	183	41	-26	5.2	33	RCMT, Soumaya et al. (2015)
12/02/1989	36.26	2.77	7	10	11	10.6	5.0	34	NEIC
29/10/1989	36.61	2.33	13	242	55	87	6.0	35	Bounif et al. (2003)
20/12/1989	37.3	-7.3	23	351	77	10	5.0	36	Buform et al. (2004)
15/11/1992	35.73	1.15	7	274	70	-169	5.0	37	Harvard CMT
23/04/1993	35.27	-2.42	6	308	86	4	5.4	38	Bezzeghoud and Buform (1999)
23/05/1993	35.27	-2.42	6	308	86	4	5.4	39	Bezzeghoud et al. (2012, 2014)
23/12/1993	36.77	-2.99	8	300	70	-130	5.4	40	Buform et al. (2004)
26/05/1994	35.14	-3.92	7	330	77	-45	5.3	41	Bezzeghoud and Buform (1999)
26/05/1994	35.16	-3.92	8	355	69	2.5	5.7	42	Bezzeghoud and Buform (1999)
18/08/1994	35.6	0.36	4	58	45	95	5.7	43	Bezzeghoud and Buform (1999)
17/09/1994	36.46	9.17	10	181	47	20	5.6	44	Bahroumi et al. (2014), Soumaya et al. (2015)
22/09/1995	35.36	8.2	10	173	41	-8	5.0	45	Harvard CMT
04/09/1996	36.98	2.88	14	260	70	108	5.5	46	Stich et al. (2003)
02/02/1999	38.1	-1.5	1	125	39	56	5.1	47	Borges et al. (2001)
22/12/1999	35.34	-1.45	6	25	31	92	5.7	48	Bezzeghoud et al. (2014)

(continued)

Table 2 (continued)

Date	LAT	LON	Depth	Strike	DIP	Rate	M	n°	References
18/08/2000	35.99	4.96	10	99	71	-171	5.2	49	Harvard CMT
10/11/2000	36.60	4.773	6	251	70	97	5.7	50	Stich et al. (2003)
16/11/2000	36.65	4.759	4	254	87	88	5.2	51	Stich et al. (2003)
24/06/2002	36.03	10.29	15	28	48	128	5.2	52	Harvard CMT
21/05/2003	36.83	3.65	10	237	43	92	6.8	53	Santos et al. (2014)
21/05/2003	36.81	3.702	18	72	20	82	5.9	54	Braunmiller and Bernardi (2005)
21/05/2003	36.81	3.485	15	41	21	65	5.1	55	Braunmiller and Bernardi (2005)
22/05/2003	36.96	3.67	9	57	14	78	5.1	56	Braunmiller and Bernardi (2005)
22/05/2003	36.83	3.934	12	91	14	101	5.1	57	Braunmiller and Bernardi (2005)
27/05/2003	36.72	3.547	18	63	21	83	5.9	58	Braunmiller and Bernardi (2005)
29/05/2003	36.72	3.39	12	187	87	32	5.0	59	Braunmiller and Bernardi (2005)
02/02/2004	35.05	-3.86	10	108	73	-167	5.2	60	IAG
24/02/2004	35.13	-3.955	7	25	80	1	6.4	61	Ven der Woerd et al. (2014)
07/03/2004	35.16	-3.96	12	178	43	-43	5.1	62	Harvard CMT
04/12/2004	34.95	-2.89	12	98	61	-168	5.1	63	Harvard CMT
09/03/2005	35.62	5.707	12	22	77	-33	5.0	64	ZUR_RMT
20/03/2006	36.65	5.302	5.95	344	85	113	5.2	65	IGN
06/06/2008	35.93	-0.48	12	44	36	81	5.5	66	Harvard CMT
11/04/2010	37.1	-3.69	616.5	63	28	-39	6.3	67	GCMT
14/05/2010	35.9	4.12	12	174	77	5	5.2	68	Harvard CMT
16/05/2010	36	3.94	12	245	50	128	5.0	69	Harvard CMT
11/05/2011	37.7	-1.65	12	234	45	43	5.1	70	RCMT
25/04/2012	36.53	1.65	10	103	71	-174	5.0	71	Harvard CMT
28/11/2012	36.71	5.1	12	152	73	-170	5.0	72	RCMT

(continued)

Table 2 (continued)

Date	LAT	LON	Depth	Strike	DIP	Rake	M	n°	References
19/05/2013	36.59	5.19	15	149	63	-170	5.3	73	Harvard CMT
01/08/2014	36.87	3.22	10.4	101	19	109	5.3	74	Benfedda et al. (2017)
23/12/2014	36.46	3.072	10	42	58	85.9	5.1	75	CGS
26/12/2014	36.45	3.075	12	72.1	53.2	138.5	5.1	76	CGS
21/03/2015	35.7	5.57	13	107	71	-178	5.0	77	CGS

studied by numerous researchers (Deschamps et al. 1982; Ouyed et al. 1981, 1983; Philip and Meghraoui 1983; Yielding et al. 1981, 1989; Ousadou et al. 2014). The event was relocated by the International Seismological Centre (ISC) at 36.16°N – 1.40°E with a fixed depth of 10 km based on 514 station records. The Harvard CMT seismic moment is 5.07×10^{19} N m (M_w 7.1). The mainshock mechanism constructed using P -wave polarities at teleseismic distances shows reverse faulting along a plane striking $\text{N}45^{\circ}\text{E}$ and dipping $\text{N}54^{\circ}$ with an 83° slip angle (Ouyed et al. 1981; Deschamps et al. 1982), which is similar to the Harvard CMT solution (azimuth 50°N , dip 61° , slip 81°). The P and SH wave modelling show that the source consisted of two sub-events separated by 4 s (Yielding et al. 1981) (Fig. 3). This event is associated with 40-km-long surface ruptures that have been clearly mapped (King and Vita-Finzi 1981; Philip and Meghraoui 1983). Three segments are identified on the rupture zone as shown by the aftershock distribution and surface fault traces. The aftershock zone extends for a length of approximately 40 km in the NE–SW direction (Fig. 3), ranging between 5 and 14 km in depth, as given by the relocation using HypoDD by Ousadou et al. (2014). The distribution exhibits three segments, and the NE edge is leading in approximately the N–S direction.

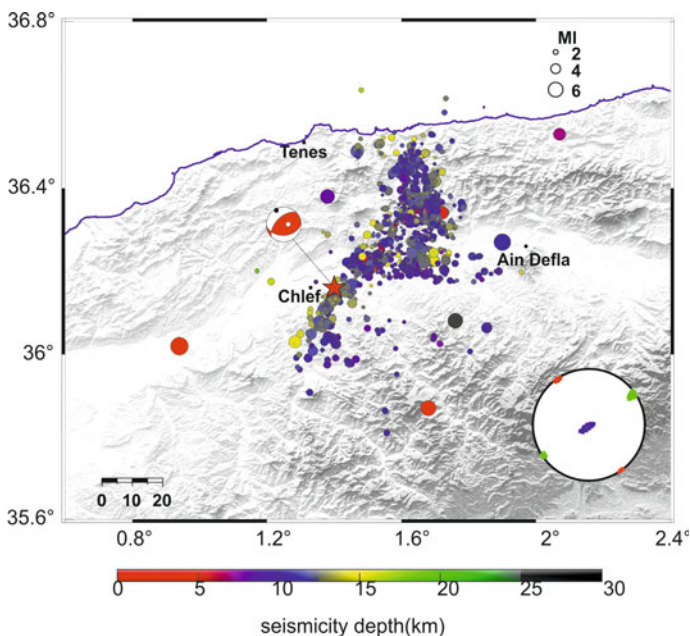


Fig. 3 The focal mechanism (Deschamps et al. 1982) and the corresponding aftershock sequence (relocated by Ousadou et al. 2014) following the mainshock of the El Asnam earthquake of 10 October 1980. Red star: mainshock after ISC relocation (2005). The regional stress tensor and principal stress (Ousadou et al. 2014) are shown in the lower right corner (Sh_{\max} in red and Sh_{\min} in blue colours). The scale bar units are in km

The focal mechanisms of the 1980 El Asnam aftershocks are well constructed using the P arrivals (Ouyed et al. 1983; Yielding et al. 1989). Most of the focal solutions for the aftershocks show reverse faulting along the El Asnam rupture zone, with an important strike–slip component both northeast and southwest of the fault. The aftershock focal mechanisms are inverted to calculate the stress field for the Cheliff basin yielding a reverse tensor with maximum and minimum horizontal stress Sh_{\max} and Sh_{\min} striking in the $N325^\circ$ and $N235^\circ$ directions, respectively (Ousadou et al. 2014). This is in good agreement with the directions of the P and T axes of the mainshock (Fig. 3).

The Cheliff basin experienced the 9 September 1954 Orléansville earthquake, which had a magnitude of M_s 6.7, maximum intensity of I_0 X (Mercalli scale) and macroseismic depth of approximately 9 km (Rothé 1955; Rothé et al. 1977). According to Heezen and Ewing (1955), breaks in submarine cables were caused by the motion of a mass of sediments detached from the continental slope by the mainshock of 1954 and transformed into a strong turbidity current. All of the focal mechanisms established from the P arrivals show reverse solutions with a fault plane dipping to the NW (Shirokova 1967; McKenzie 1972; Espinosa and Lopez 1984), which is not much different from the El Asnam one. Referring to the work of Dewey (1990), the 1954 earthquake was relocated by the Joint Epicenter Determination method, taking the 1980 earthquake near the central segment of the El Asnam fault as the reference. As a result, Dewey proposes a model of the 1954 fault, associated with the 1980 thrust fault. This model agrees with the dislocation model proposed by Bezzeghoud et al. (1995) deduced from geodetic measurements.

3.2 *The Constantine Earthquake of 27 October 1985*

The eastern part of Algeria experienced a moderate-sized earthquake (M_w 5.9) on 27 October 1985 at 18 h 34 min (TU) (Table 1). It was the strongest earthquake recorded in the Tell Atlas in the 5 years following the 1980 El Asnam earthquake. The mainshock has been relocated and showed a remarkable jump of the epicentre from outside the cloud of aftershocks (Bounif et al. 1987) to inside it (Ousadou et al. 2013). The focal solution using P and SH waveform inversions shows a left-lateral strike–slip mechanism on a fault striking $N217^\circ$ and dipping 84° with a rake of 19° , a depth fixed at 9 km and a seismic moment of 5.2×10^{17} N m (Deschamps et al. 1991).

The aftershocks have been located (Bounif and Dorbath 1998) and, once more, relocated in a 3D model using TomoDD (Ousadou et al. 2013). The aftershock relocation by TomoDD is better defined and less scattered than that of the 1980 El Asnam earthquake (Fig. 4). It extends for a length of approximately 30 km, but only the 14-km-long central part shows an alignment in the $N210^\circ/215^\circ$ direction, which corresponds to one of the two nodal planes given by Harvard CMT (2005) and Deschamps et al. (1991). This segment extending from 5 to 15 km down has been subsequently interpreted as the source of the mainshock rupture, and the

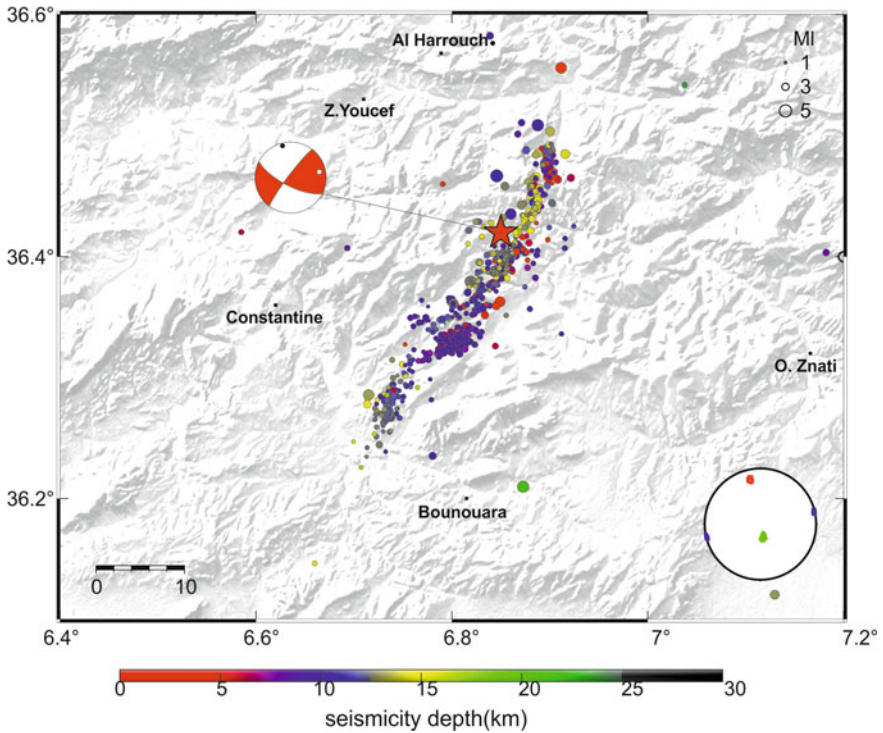


Fig. 4 The focal mechanism (Deschamps et al. 1991) and the corresponding aftershock sequence (relocated by Ousadou et al. 2013) following the mainshock of the Constantine earthquake of 27 October 1985. Red star: main shock after relocation (Ousadou et al. 2014). The regional stress tensor and principal stress (Ousadou et al. 2014) are shown in the lower right corner (Sh_{max} in red and Sh_{min} in green colours). The scale bar units are in km

4.5-km-long surface breaks, organized in an *en échelon* system, are secondary ruptures due to ground shaking around the epicentral area (Ousadou et al. 2013).

The aftershock focal mechanisms have been manually constructed, and the majority of them exhibit strike-slip faulting with some reverse or normal components, located between 10- and 15-km depths and spread all along the seismic zone (Ousadou et al. 2013). The inversion of aftershock focal mechanisms yields a strike-slip tectonic regime with quasi-horizontal Sh_{max} and Sh_{min} striking in the N347° and N257° directions, respectively. This is in accordance with the tectonic observations made in the Constantine basin, which is defined by the left-lateral strike-slip character of the NE-SW trending Ain Smara fault (Fig. 4). The Sh_{max} and Sh_{min} orientations correspond to the P and T axes of the mainshock mechanism (Ousadou et al. 2014).

3.3 The Tipasa–Chenoua Earthquake of 29 October 1989

The moderate earthquake that occurred on 29 October 1989 with magnitude M_s 5.9 struck the northwestern part of the Mitidja basin in the locality of Tipasa–Chenoua at 19 h 09 min (TU) (Table 1). The mainshock was located by NEIC and relocated by Bounif et al. (2003) (Fig. 5). The P and SH body wave modelling reveals almost pure reverse faulting along a plane striking 246°N and dipping 56° with an 86° slip angle and a seismic moment of 8.2×10^{17} N m, M_w 6.0 (Bounif et al. 2003) (Fig. 5).

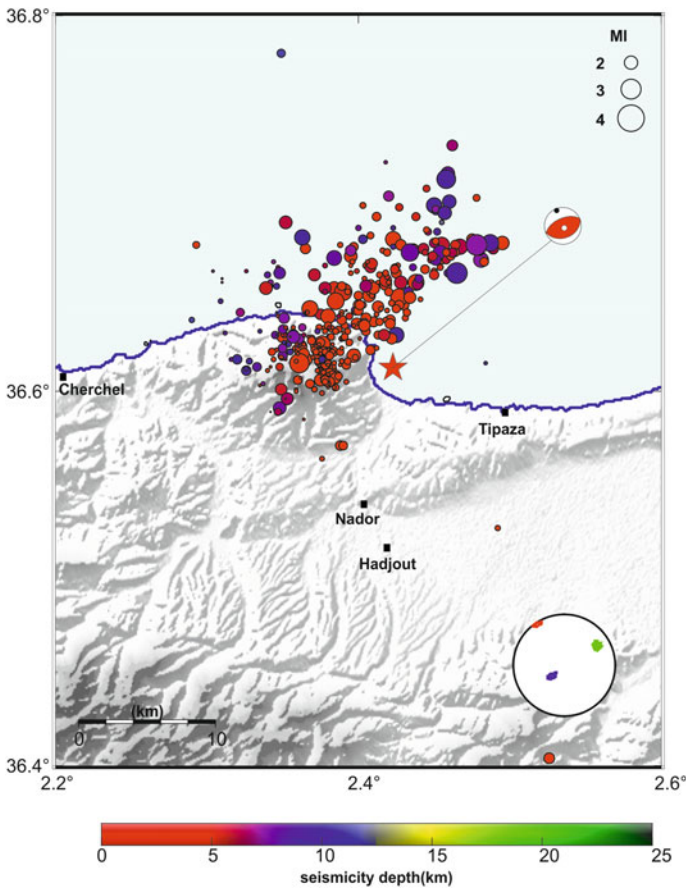


Fig. 5 The focal mechanism (Bounif et al. 2003) and the corresponding aftershock sequence (relocated by Ousadou et al. 2014) following the mainshock of the Tipasa–Chenoua earthquake of 29 October 1989. Red star: mainshock after relocation (Bounif et al. 2003). The regional stress tensor and principal stress (Ousadou et al. 2014) are shown in the lower right corner ($S_{h_{max}}$ in red and $S_{h_{min}}$ in blue colours)

The epicentral distribution of the aftershocks depicts an elongated area with a general SW–NE direction approximately 15 km long and 7 km wide. Most of these aftershocks lie offshore, and there is no clear segmentation of the aftershock zone (Fig. 5).

The aftershock focal solutions reconstructed manually (Ousadou et al. 2014) show predominantly pure reverse faulting with a weak left-lateral strike–slip component on a plane dipping to the NW and striking NE–SW. This is in agreement with the geometry of the aftershock area and the focal mechanism of the mainshock (Fig. 5).

The set of aftershock focal mechanisms has been inverted to calculate a compressive stress tensor with well-defined horizontal Sh_{\max} and Sh_{\min} trending N326° and N239°, respectively (Ousadou et al. 2014). These two directions are close to those of the P and T axes of the mainshock focal solution and very close to that obtained in Chelif Basin, located approximately 100 km southwestward.

3.4 *The Mascara Earthquake of 18 August 1994*

The Oranie region (northwestern Algeria) has experienced several significant earthquakes in the last centuries; the most important one is that of Oran city on February 9, 1790, $I_o = XI$, which destroyed the town completely and caused the loss of many lives. Since 1790, no other event has been as disastrous, except that of 18 August 1994, with a magnitude of M_w 5.7 (Ayadi et al. 2002), which struck Mascara Province (Algeria) at 01 h 13 min GMT (Table 1). The Mascara earthquake is located in a zone with low seismic activity but with a maximum intensity I_o of IX from past earthquakes (Ayadi and Bezzeghoud 2015). However, since the beginning of this century, the region has been dominated by seismic quiescence, and no event with magnitude larger than 5.5 has occurred in this area.

The focal solutions computed by Harvard, Bezzeghoud and Buforn (1999) using waveform modelling and Thio et al. (1999) using single station inversion (hybrid method), show a reverse mechanism on a single rupture striking in the NE–SW direction at a shallow depth (4.5 km) and a scalar seismic moment of 3.3×10^{17} N m. These focal mechanisms seem to be in good agreement with the tectonic observations (Thomas 1985) and with the macroseismic map (Ayadi et al. 2002).

3.5 *The Ain Temouchent Earthquake of 22 December 1999*

The Ain Temouchent region situated in the northwestern part of Algeria is characterized by low-to-moderate seismic activity in comparison with the Oran and Mascara regions. Nevertheless, the region was shaken on 22 December 1999, by an earthquake of magnitude M_w 5.7 (Table 1). The focal mechanism of the mainshock

has been established using broadband data at regional and teleseismic distances (Yelles-Chauouche et al. 2004), and the scalar seismic moment estimated from waveform modelling is 4.7×10^{17} N m. Unfortunately, there is no aftershock study for this earthquake.

Indeed, throughout history, no important earthquakes have been mentioned in the seismic catalogues for this region (Fig. 1) (Roussel 1973; Benhallou 1985; Mokrane et al. 1994; Benouar 1994; Ayadi and Bezzeghoud 2015). These catalogues all indicate a low level of seismic activity with the occurrence of earthquakes having magnitudes less than 5.5. The Ain Temouchent earthquake is the largest seismic event ever recorded in the region with a maximum observed intensity of VII (MSK scale).

3.6 The Zemmouri—Boumerdes Earthquake of 21 May 2003

The easternmost edge of the Mitidja Basin experienced a strong earthquake of M_w 6.8 on 21 May 2003, at 18 h 44 min (TU), located to the east of the city of Algiers; this was the largest seismic event felt since that of 3 February 1716, which had $I_o = X$ (Rothé 1950; Harbi et al. 2015) (Table 1). The Zemmouri—Boumerdes earthquake occurred along the complex thrust and fold system of the Tell Atlas in the northeastern continuation of the Blida Mountain front and the related Mitidja Quaternary Basin.

Bounif et al. (2004) relocated the mainshock hypocenter, using three major aftershocks, with results that show a shift of this hypocenter from offshore to the coastline at 8–10 km depth. This coastal epicentre suggests a rupture along a previously unidentified offshore fault. According to Ayadi et al. (2003), this fault is an offshore continuation of the south Mitidja fault system. This is also supported by field observations of coastal uplift marked by a continuous white band of some sort of deposit attributed to a period of uplift, which is visible in exposed cliff faces (Meghraoui et al. 2004). Geodetic measurements of the 50-km-long coast show an average uplift of approximately 0.55 m along the shoreline with a maximum of 0.75 m east of Boumerdes and a minimum close to 0 near Cap Djenet (Meghraoui et al. 2004).

According to the study on teleseismic waveform inversion performed by Delouis et al. (2004), the Zemmouri—Boumerdes event was associated with an SE-dipping thrust fault mechanism with a seismic moment of 2.86×10^{19} N m (M_w 6.9), implying a 50-km-long fault rupture that should appear on the sea bottom at 6–12 km offshore from the coast (Fig. 6). Santos et al. (2015) investigate the rupture process to shed light on the location and geometry of the seismic fault and slip distribution using methodology based on teleseismic data, uplift measurements and synthetic aperture radar data. The methodology used by Santos et al. (2015) processes the available seismic and geodetic data to evaluate the two

complementary planes of the focal mechanism. The location and geometry of the model proposed by Santos et al. (2015) are in agreement with the aftershock relocation proposed by Ayadi et al. (2008), where one aftershock cloud corresponded to a fault that dipped to the SE.

The event was followed by a large sequence of aftershocks. More than 900 aftershocks that were relocated with TomoDD extend NE–SW along an approximately 60-km-long zone crossing the coastline and exhibit at least three seismic clouds and a well-defined SE-dipping main fault geometry (Ayadi et al. 2008). The distribution of seismic events presents a clear contrast between a dense SW zone and a NE zone with scattered aftershocks (Fig. 6).

The aftershock focal mechanisms were determined by inverted seismic broadband (Braunmiller and Bernardi 2005) and constructed using *P*-wave onsets (Ayadi et al. 2008; Ousadou et al. 2014). The majority of the solutions are reverse mechanisms, similar to the mainshock and two of the three largest aftershocks. However, at the eastern extremity of the seismic cloud, some events show reverse faulting on planes striking approximately N–S. Some strike–slip and normal faulting solutions are found, especially at the westernmost end of the aftershock cloud (Ousadou et al. 2014).

The aftershock focal mechanism database was inverted to calculate the stress tensor for the eastern part of the Mitidja basin, which is a compressive stress triaxial tensor with well-defined horizontal Sh_{\max} and Sh_{\min} in the $N340^\circ$ and $N251^\circ$ directions, respectively (Ousadou et al. 2014).

4 The Impact of Earthquakes in Algeria

Earthquakes are the expression of the dispersion of energy through seismic waves. The quantification of this seismic energy led seismologists to define different magnitudes. Several energy–magnitude empirical relations have been determined, the most suitable ones being those proposed by Gutenberg and Richter (1956), which express, in this study, the energy in joule from the magnitudes m_b , and M_s given by the formulas $\log E = 2.4m_b - 1.2$ and $\log E = 1.5M_s + 4.8$, respectively, as well as the relationship established by Kanamori (1977) giving the energy in joules from the moment magnitude M_w by the same formula that for M_s . However, to calculate the energy released from the historical earthquakes (1365–1900) we use Mokrane et al. (1994) empirical relation which is the magnitude versus intensity: $M_m = 0.97I_o - 2.24$ for $IX < I_o \leq XI$.

Based on the catalogue of Ayadi and Bezzeghoud (2015) and using the formulas above, we estimated the seismic energy released by the 23 earthquakes with $M > 5.5$ that occurred in Algeria during the period between 1900 and 2015 (Fig. 1). The results show that 69% of the total energy (Fig. 7) comes from the El Asnam earthquake of 10 October 1980 (indicated by a red star in Fig. 4), if we consider that its magnitude was M_s 7.3. The El Asnam earthquake is the seismic event that dominates all the seismicity of the region for this period (1900–2015). A more

recent earthquake that occurred in the Zemmouri—Boumerdes region on 21 May 2003 with a magnitude M_w 6.8 (Fig. 6) represents only 12% of the total energy (Fig. 7) released by the earthquakes occurring in the same period (1900–2015). Meanwhile, the other five recent earthquakes discussed in the previous sections released very low amounts of energy (1%, Fig. 7) when compared with the total seismic energy released by the El Asnam earthquake of 10 October 1980.

However, for the total period (1365–2015) listed in the catalogue of Ayadi and Bezzeghoud (2015), the seismic energy released by the El Asnam earthquake of 10 October 1980 and the Zemmouri—Boumerdes earthquake of 21 May 2003, at 8 and 1%, respectively, is much less significant when compared to that released (88%) (Fig. 8) by the six major historical earthquakes (2 January 1365; 9 October 1790; March 1819; 2 March 1825; 2 January 1867 and 1 January 1891) (Fig. 1). The other seven recent earthquakes discussed in the previous sections released an insignificant amount of energy (<1%, Fig. 8) when compared with the total seismic energy released by all the seismic events recorded in the period 1365–2015.

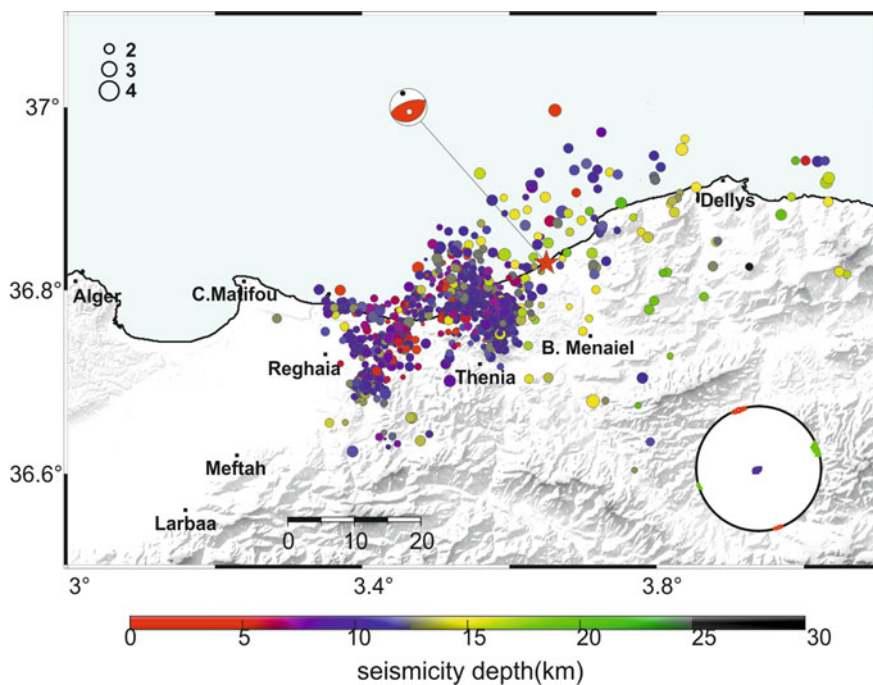


Fig. 6 The focal mechanism (Braunmiller 2005) and the corresponding aftershock sequence (relocated by Ayadi et al. 2008) following the mainshock of the Zemmouri—Boumerdes earthquake of 21 May 2003. Red star: mainshock after relocation (Bounif et al. 2004). The regional stress tensor and principal stress (Ousadou et al. 2014) are shown in the lower right corner (Sh_{max} in red and Sh_{min} in blue colours). The scale bar units are in km

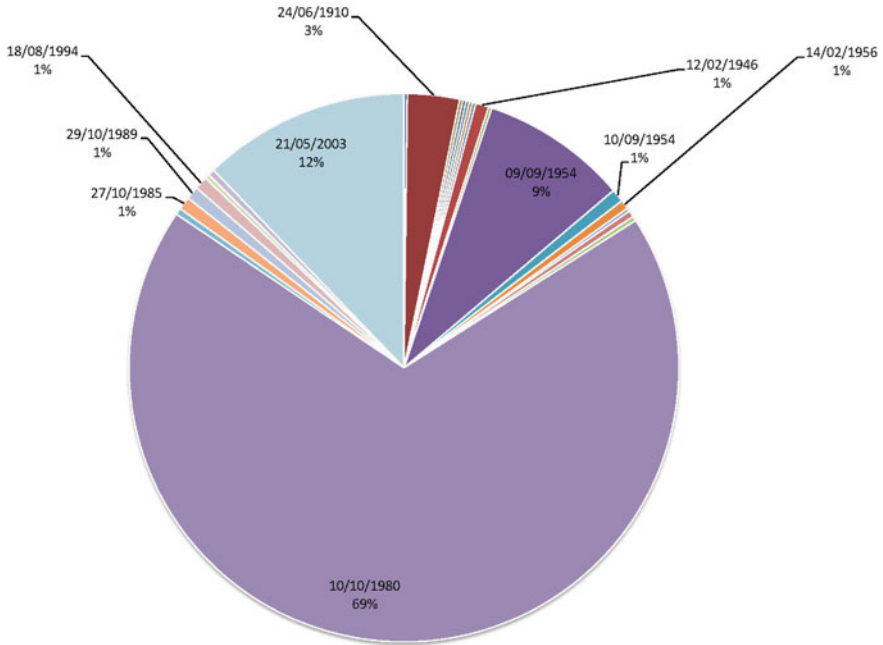


Fig. 7 Diagram representing the percentage of seismic energy released by the earthquakes occurred in Algeria for the period 1900–2015 based on the catalogue of Ayadi and Bezzeghoud (2015). Note that the El Asnam earthquake of 10 October 1980 represents 69% of the total seismic energy for this period. See text for details

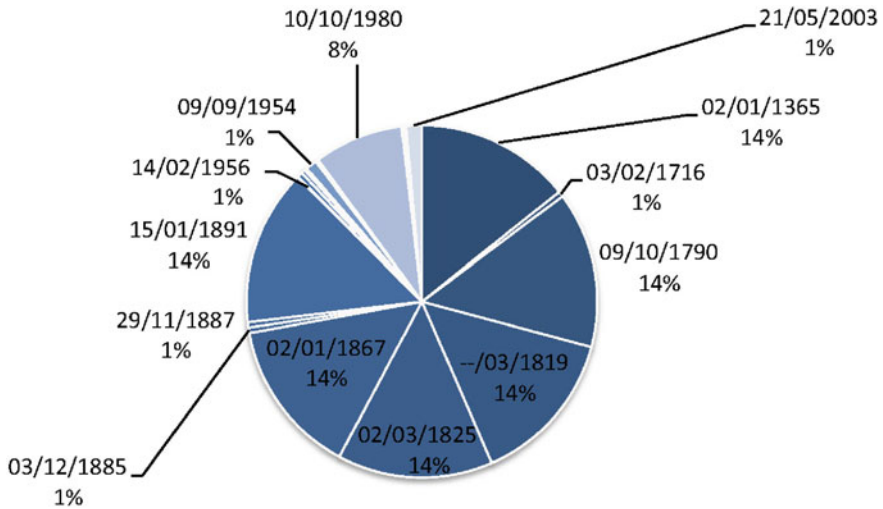


Fig. 8 Diagram representing the percentage of seismic energy released by the earthquakes occurring in Algeria for the period 1365–2015 based on the catalogue of Ayadi and Bezzeghoud (2015). Note that the six major historical earthquakes (02/01/1365; 09/10/1790; 03/1819; 02/03/1825; 02/01/1867 and 15/01/1891) (see Fig. 1) represent 84% of the total seismic energy for this period. See text for details

5 Discussion and Conclusion

Generally, northern Africa has experienced moderate to strong earthquakes. However, between 1920 and the present, three earthquakes with magnitudes of approximately 8.0 occurred in the oceanic region (M_w 8.2, 25 November 1941; M_s 8.0, 28 February 1969; M_w 7.9, 26 May 1975), and four earthquakes with magnitudes of approximately 7.0 (M_w 7.1, 8 May 1939, Santa María Island; M_w 7.1, 1 January 1980, Azores; M_s 7.1, 20 May 1931, Azores–Gibraltar fracture zone; M_w 7.3, 10 October 1980, El Asnam, Algeria) occurred along the western part of the Eurasian–Nubian plate boundary (Bezzeghoud et al. 2014). In general, the major earthquakes ($M \geq 7.0$) have occurred within the oceanic region, except for the El Asnam (Algeria) earthquake. The deadliest earthquakes that occurred in the study area since 1920, measured in numbers of victims, were those recorded in El Asnam, north Algeria (1954 and 1980), Azores, Portugal (1980 and 1998), Al Hoceima, north Morocco (1994 and 2004) and Zemmouri—Boumerdes, north Algeria (2003) (Benouar 1994; Bezzeghoud et al. 1996, 2014; Bezzeghoud and Buform 1999; Ayadi et al. 2003).

The Ibero-Maghrebian region is vulnerable due to the shallow character of its seismicity generated by the convergence of the Eurasian and Nubian tectonic plates, to the specific mechanical properties of the crust and to local site effects (Bezzeghoud and Buform 1999; Mourabit et al. 2014). To lead to a better assessment of the hazards and risks in and around urban areas, we need to know the detailed behaviour of the fault rupture processes that cause the earthquakes. Next, to produce reliable seismic hazard maps and mitigate the destructive impact of the earthquakes, the regional seismic hazards must be assessed using different approaches (e.g. deterministic and probabilistic) based on available historical and instrumental seismicity data (Ayadi and Bezzeghoud 2015; Harbi et al. 2015), earthquake sources and seismotectonic zoning studies and structural models associated with attenuation laws (Mourabit et al. 2014).

In summary, Algeria presents a seismotectonically complex area in which earthquakes responsible for high social and economic impacts have occurred and will continue to occur in the future. An Earthquake Early Warning System (EEWS) for this zone could be very useful in mitigating the damage caused by large earthquakes (Buform et al. 2015). The complexity of the Ibero-Maghrebian region results in the need to address in depth the problem of the design of the early warning network to develop an appropriate EEWS. One of the issues that is particularly important is whether a single alert system could effectively cover the entire region or whether more than one system would be required instead, which takes into consideration the different seismic behaviours found in the areas under study. A preliminary feasibility study for an EEWS in the Gulf of Cadiz was performed as part of the ALERT-ES project coordinated by the Complutense University of Madrid with the participation of the Royal Institute and Naval Observatory of San Fernando, Cádiz, the Geological Institute of Catalonia in Barcelona and the

University of Évora. The extension of this system to the entire Ibero-Maghrebian region is now in progress with the ALERTE-RIM project, which began in 2015 with the same participants.

Data and resources

Data are available from the literature listed in the references section and from (1) the GCMT, Global Centroid Moment Tensors: <http://www.globalcmt.org>; (2) Harvard CMT (2005) Centroid Moment Tensor Project: <http://www.globalcmt.org/CMTsearch.html>; (3) IAG, Instituto Andaluz de Geofísica: <http://www.iagpds.ugr.es>; (4) IGN (2004), Instituto Geográfico Nacional, Spanish seismic network: <http://www.ign.es/ign/en/IGN/home.jsp>; (5) ISC (2008), International Seismological Centre: <http://www.isc.ac.uk>, Internat. Seis. Cent., Thatcham, United Kingdom; (6) NEIC, National Earthquake Information Center: <http://neic.usgs.gov>; (7) RCMT, Regional Centroid Moment Tensors: <http://www.bo.ingv.it/RCMT>; and (8) ZUR_RMT, Swiss Seismological Service (SED): <http://www.seismo.ethz.ch/en/>. Topography and bathymetry data have been extracted from the GEBCO (General Bathymetric Chart of the Oceans: <http://www.gebco.net>).

Acknowledgements This study was conducted within the scope of the MEDYNA FP7-PEOPLE-2013-IRSES project, WP-1: Present-day Kinematics and seismic hazards, funded by the Seventh Framework European Programme. The authors acknowledge the support provided by the Instituto de Ciências da Terra da Universidade de Évora (Portugal) and the Centre de Recherche en Astronomie, Astrophysique et Géophysique (Algiers, Algeria), under contract with the Portuguese Science and Technology Foundation (FCT, Portugal), PEst-OE/CTE/UI0078/2011. We would like to thank the Editors, Prof. Abderrahmane Bendaoud and Prof. Mohamed Hamoudi (Algiers University, USTHB), for their help.

References

- Abbes K, Dorbath L, Dorbath C, Djeddi M, Ousadou F, Maouche S, Benkaci N, Slimani A, Larbes L, Bouziane D (2016) The Beni Haoua, Algeria, Mw 4.9 earthquake: source parameters, engineering, and seismotectonic implications. *J Seismolog* 20(2):655–667. <https://doi.org/10.1007/s10950-015-9549-1>
- Ayadi A, Bezzeghoud M (2015) Seismicity of Algeria from 1365 to 2013: maximum observed intensity map (MOI2014). *Seismol Res Lett* 86(1). <https://doi.org/10.1785/0220140075>
- Ayadi A, Ousadou-Ayadi F, Bourouis S, Benhallou H (2002) Seismotectonic and seismic quietness of the Oranie region (western Algeria); the Mascara earthquake of August 18th 1994, Mw = 5.7, Ms = 6.0. *J Seismolog* 6(1):13–23
- Ayadi A, Maouche S, Harbi A, Meghraoui M, Beldjoudi H, Oussadou F, Mahsas A, Benouar D, Heddar A, Rouchiche Y, Kherroubi A, Frogneux M, Lammali K, Benhamouda F, Sebai A, Bourouis S, Alasset PJ, Aoudia A, Cakir Z, Merahi M, Nouar O, Yelles A, Bellik A, Briole P, Charade O, Thouvenot F, Semane F, Ferkoul A, Deramchi A, Haned SA (2003) Strong Algerian earthquake strikes near capital city. *Eos Trans Am Geophys Union* 84:561–568
- Ayadi A, Dorbath C, Ousadou F, Maouche S, Chikh M, Bounif MA, Meghraoui M (2008) Zemmouri earthquake rupture zone (Mw 6.8, Algeria): aftershocks sequence relocation and 3D velocity model. *J Geophys Res Solid Earth* 113(B9):B09301. <https://doi.org/10.1029/2007JB005257>

- Bahrouni, Soumaya, Ben Ayed N, Bouaziz S, Attafik K, Rebai (2013) Investigation of historical seismicity in Tunisia from the records of building damage. In: The large Mediterranean earthquakes from past to present-international symposium, Algiers, 21–23 May 2013, Abstracts vol
- Bahrouni N, Bouaziz S, Soumaya A, Ben Ayed N, Attafi K, El Ghali A, Rebai N (2014) Neotectonic and seismotectonics investigation of seismically active regions in Tunisia: a multidisciplinary approach. *J Seismolog* 18:235–256. <https://doi.org/10.1007/s10950-013-9395-y>
- Ben Ayed N, Zargouni F (1990) Carte sismotectonique de la Tunisie à l'échelle 1/1000 000. Fondation Nationale de la Recherche Scientifique, Tunisia
- Benhallou (1985) Les catastrophes séismiques de la région d'Echlllef dans le contexte de la sismicité Historique de l'Algérie. Thèse de Doctorat Es-Sciences, IST-USTHB, Alger, Algérie
- Benouar D (1994) Materials for investigation of the seismicity of Algeria and adjacent regions during the twentieth century. *Ann Geophys* 37(4)
- Benfedda A, Abbes K, Bouziane D, Bouhadad Y, Slimani A, Larbes S, Haddouche D, Bezzeghoud M (2017) The August 1st, 2014 (Mw 5.3) Moderate earthquake: evidence for an active thrust fault in the bay of Algiers (Algeria), *Pure Appl Geophys* 174(3):1503–1511. <https://doi.org/10.1007/s00024-017-1481-6>
- Bezzeghoud M, Buforn E (1999) Source parameters of the 1992 Melilla (Spain, Mw = 4.8), 1994 Al Hoceima (Morocco, Mw = 5.8) and Mascara (Algeria, Mw = 5.7) earthquakes and seismotectonic implications. *Bull Seismol Soc Am* 89(2):359–372
- Bezzeghoud M, Dimitrov D, Ruegg JC, Lammali K (1995) Faulting mechanism of the El Asnam (Algeria) 1954 and 1980 earthquake from modeling of vertical movements. *Tectonophysics* 249:249–266
- Bezzeghoud M, Ayadi A, Sébaï A, Aït Messaoud M, Mokrane A, Benhallou H (1996) Seismicity of Algeria between 1365 and 1989: map of maximum observed intensities (MOI). *Av Geofis Geod* 1:107–114
- Bezzeghoud M, Borges JF, Caldeira B, Buforn E, Udias A (2008) Seismic activity in the Azores region in the context of the western part of the Eurasia–Nubia plate boundary. In: International seminar on seismic risk and rehabilitation on the 10th anniversary of the July 9 1998 Azores earthquake, Horta-Azores, 9–13 July, pp 27–31
- Bezzeghoud M, Borges JF, Caldeira B (2012) Fontes sísmicas ao longo da fronteira de placas tectónicas entre os Açores e a Argélia: um modelo sismotectónico. In: Dias R, Araújo A, Terrinha P, Kullberg JC (eds) *Geologia de Portugal*, vol 2. Escolar Editora, pp 747–790. ISBN: 978-972-592-364-1
- Bezzeghoud M, Adam C, Buforn E, Borges JF, Caldeira B (2014) Seismicity along the Azores-Gibraltar region and global plate kinematics. *J Seismolog* 18:205–220. <https://doi.org/10.1007/s10950-013-9416-x>
- Borges JF, Fitas AJS, Bezzeghoud M, Teves-Costa P (2001) Seismotectonics of Portugal and its adjacent Atlantic area. *Tectonophysics* 337:373–387
- Borges JF, Bezzeghoud M, Buforn E, Pro C, Fitas AJS (2007) The 1980, 1997 and 1998 Azores earthquakes and its seismotectonic implications. *Tectonophysics* 435:37–54
- Borges JF, Caldeira B, Bezzeghoud M, Buforn E (2008) Seismicity and seismotectonics of Azores: geodynamic implications. In: Oliveira CS, Costa A, Nunes JC (eds) *A book on the 1998 Azores earthquake—10 years after its occurrence*, pp 99–110. ISBN 978.989-20-1223-0, 741 p
- Bouaziz S, Barrier E, Soussi M, Turki MM, Zouari H (2002) Tectonic evolution of the northern African margin in Tunisia from paleostress data and sedimentary record. *Tectonophysics* 357:227–253
- Bouhadad Y, Nour A, Laouami N, Behai D (2003) The Tachauaft-Beni-ourtilane fault and seismotectonic aspects of the Babors region (eastern Algeria). *J Seismolog* 7:79–88. <https://doi.org/10.1023/A:1021259931865>

- Bouhadad Y, Benhamouche A, Bourenane H, Ait ouali A, Chikh M, Guessoum N (2010) The Laalam (Algeria) damaging landslide triggered by a moderate earthquake (Mw = 5.2). *J Nat Hazards* 54:261–272
- Bounif MA, Dorbath C (1998) Three-dimensional velocity structure and relocated aftershocks for the 1985 Constantine, Algeria (Ms = 5.9) earthquake. *Ann Geophys* 41(1):93–104
- Bounif MA, Haessler H, Meghraoui M (1987) The Constantine (Northeast Algeria) earthquake of October 27, 1985; surface ruptures and aftershock study. *Earth Planet Sci Lett* 85(4):451–460. [https://doi.org/10.1016/0012-821X\(87\)90140-3](https://doi.org/10.1016/0012-821X(87)90140-3)
- Bounif A, Bezzeghoud M, Dorbath L, Legrand D, Deschamps A, Rivera L, Benhallou H (2003) Seismic source study of the 1989, October 29, Chenoua (Algeria) earthquake from aftershocks, broad-band and strong motion records. *Ann Geophys* 46(4):625–646
- Bounif A, Dorbath C, Ayadi A, Meghraoui M, Beldjoudi H, Laouami N, Frogneux M, Slimani A, Alasset PJ, Kharroubi A, Ousadou F, Chikh M, Harbi A, Larbes S, Maouche S (2004) The 21 May Zemmouri (Algeria) earthquake Mw 6.8: relocation and aftershock sequence analysis. *Geophys Res Lett* 31:L19606. <https://doi.org/10.1029/2004gl020586>
- Braunmiller J, Bernardi F (2005) The 2003 Boumerdes, Algeria earthquake: regional moment tensor analysis. *Geophys Res Lett* 32(6):L06305. <https://doi.org/10.1029/2004GL022038>
- Buform E (2008) Seismotectonics of Azores-Tunisia. In: Mendes-Victor L, Sousa Oliveira C, Azevedo J, Ribeiro A (eds) *The 1755 Lisbon earthquake revisited*, pp 397–410
- Buform E, Udías A, Madariaga R (1991) Intermediate and deep earthquakes in Spain. *Pure Appl Geophys* 136:375–393
- Buform E, Bezzeghoud M, Udías A, Pro C (2004) Seismic sources on the Iberia-African plate boundary and their tectonic implications. *Pure Appl Geophys* 161(3):623–646
- Buform E, Udías A, Pro C (2015) Large earthquakes at the Ibero-Maghrebian region. Basis for an EEWS. *Pure Appl Geophys* 172(2015):2387–2396. <https://doi.org/10.1007/s00024-014-0954-0>
- Buform E, Pro C, de Galdeano CS, Cantavella JV, Cesca S, Caldeira B, Udías A, Mattesini M (2017) The 2016 south Alboran earthquake (Mw = 6.4): a reactivation of the Ibero-Maghrebian region? *Tectonophysics* 712:704–715. <http://www.sciencedirect.com/science/article/pii/S0040195117302792>
- De Vicente G, Cloetingh S, Munoz-Martin A, Olaiz A, Stich D, Vegas R, Galindo-Zaldívar J, Fernandez-Lozano J (2008) Inversion of moment tensor focal mechanisms for active stresses around the micro-continent Iberia: tectonic implications. *Tectonics* 27:TC1009. <https://doi.org/10.1029/2006tc002093>
- Delouis B, Vallée M, Meghraoui M, Calais E, Maouche S, Lammali K, Mahsas A, Briole P, Benhamouda F, Yelles K (2004) Slip distribution of the 2003 Boumerdes-Zemmouri earthquake, Algeria, from teleseismic, GPS, and coastal uplift data. *Geophys Res Lett* 31
- Deschamps A, Gaudemer Y, Cisternas A (1982) The El Asnam, Algeria, earthquake of October 1980: multiple-source mechanism determined from long-period records. *Bull Seismol Soc Am* 72(4):1111–1128
- Deschamps A, Bezzeghoud M, Bounif A (1991) Seismological study of the Constantine (Algeria) earthquake (27 October 1985). In: Mezcuca J, Udías A (eds) *Seismicity, seismotectonics and seismic risk of the Ibero-Maghrebian region*, vol 8. Publ. IGN. Madrid, pp 163–173
- Dewey (1990) The 1954 and 1980 Algerian earthquakes: implications for the characteristic-displacement model of fault behavior. *Bull Seismol Soc Am* 81(2):446–467
- El Mrabet T (2005) *The great earthquakes in the Maghreb region and their consequences on man and environment*, (in Arabic with abstract in English). Edit Centre National de Recherche Scientifique et Technique, Rabat, Morocco
- Espinoza AF, Lopez-Arroyo A (1984) Inconsistencies in the modified Mercalli intensities scales, El Asnam, Algeria, earthquake. In: *Proc Conf Int Sur la microzonation sismique*, Ech Cheliff, Algeria, 10–12 Oct 1984, pp 51–65
- Gueddiche M, Harjono H, Ben Ayed N, Hfaiedh M, Diamant M, Dubois J (1992) Analyse de la sismicité et mise en évidence d'accidents actifs dans le nord de la Tunisie. *Bull Soc Geol Fr* 163:415–425

- Gutenberg B, Richter CF (1956) Earthquake magnitude, intensity, energy and acceleration. *Bull Seismol Soc Am* 46:105–145
- Gutscher MAS, Dominguez GK, Westbrook P Le, Roy F Ros (2012) The Gibraltar subduction: a decade of new geophysical data. *Tectonophysics* 574–575(2012):72–91
- Harbi A, Maouche S, Ayadi A (1999) Neotectonics and associate seismicity in the eastern Tellian Atlas of Algeria. *J Seismolog* 3(1):95–104
- Harbi A, Peresan A, Panza GF (2010) Seismicity of eastern Algeria: a revised and extended earthquake catalogue. *Nat Hazards* 54(3):725–747. <https://doi.org/10.1007/s11069-009-9497-6>
- Harbi A, Sebaï A, Benmedjber M, Ousadou F, Rouchiche R, Grigahcene A, Aïni D, Bourouis S, Maouche S, Ayadi A (2015) The Algerian homogenized macroseismic database (267–1989): a deeper insight into the Algerian historical seismicity. *Seismol Res Lett* 86:6. <https://doi.org/10.1785/0220150092>
- Hatzfeld D (1978) Étude sismotectonique de la zone de collision Ibero-Maghrébine. Ph.D. thesis, Grenoble (France), 281 pp
- Heezen BC, Ewing M (1955) Orleansville earthquake and turbidity currents. *AAPG Bull* 39(12): 2505–2514
- Henares J, López Casado C, Sanz de Galdeano C, Delgado J (2003) Stress fields in the Iberian-Maghrebi region. *J Seismolog* 7(1):65–78. <https://doi.org/10.1023/A:1021294015027>
- Hfaïedh M, Ben Ayed N, Dorel J (1985) Etude néotectonique et sismotectonique de la Tunisie nord-orientale. *Note Serv Géol Tunisie* n 16, pp 41–56
- Houseman G (1996) From mountains to basins. *Nature* 379:771–772
- Kanamori H (1977) The energy release in great earthquakes. *J Geophys Res* 82(20):2981–2987. <https://doi.org/10.1029/JB082i020p02981>
- King GCP, Vita-Finzi C (1981) Active folding in the Algerian earthquake of 10 October 1980. *Nature* 292(5818):22–26
- Maouche S, Meghraoui M, Morhange C, Belabbes S, Bouhadad Y, Haddoum H (2011) Active coastal thrusting and folding, and uplift rate of the Sahel Anticline and Zemmouri earthquake area (Tell Atlas, Algeria). *Tectonophysics* 509:69–80. <https://doi.org/10.1016/j.tecto.2011.06.003>
- Martinez Solares JM, Mezcua Rodriguez J (eds) (2002) *Catalogo simico de la Peninsula Iberica (880 a.C.-1990)*. IGN, Madrid, Monografía Núm. 18, 254 pp
- McKenzie D (1972) Active tectonics of the Mediterranean region. *Geophys J Roy Astron Soc* 30 (2):109–185
- Meghraoui M (1988) *Géologie des zones sismiques du Nord de l'Algérie: Paléosismologie, tectonique active et synthèse sismotectonique*. Thèse de doctorat Université Pierre et Marie Curie, France, p 356
- Meghraoui M, Maouche S, Chemaï B, Cakir Z, Aoudia A, Harbi A (2004) Coastal uplift and thrust faulting associated with the M (sub w) = 6.8 Zemmouri (Algeria) earthquake of 21 May 2003. *Geophys Res Lett* 31:L19605. <https://doi.org/10.1029/2004GL020466>
- Mokrane A, Aït Messaoud A, Sebaï A, Menia A, Ayadi A, Bezzeghoud M (1994) Les séismes en Algérie de 1365 à 1992. In: Bezzeghoud M, Benhallou H (eds) *Publication du Centre de Recherche en Astronomie Astrophysique et Géophysique, Alger-Bouzaréah*, 277 p
- Mourabit T, Abou Elenean KM, Ayadi A, Benouar D, Ben Suleman A, Bezzeghoud M, Cheddadi A, Chourak M, ElGabry MN, Harbi A, Hfaïedh M, Hussein HM, Kacem J, Ksentini A, Jabour N, Magrin A, Maouche S, Meghraoui M, Ousadou F, Panza GF, Peresan A, Romdhane N, Vaccari F, Zuccolo E (2014) Neo-deterministic seismic hazard assessment in North-Africa. *J Seismolog* 18(2):301–318. <http://dx.doi.org/10.1007/s10950-013-9375-2>
- Ousadou F, Dorbath L, Dorbath C, Bounif MA, Benhallou H (2013) The Constantine (Algeria) seismic sequence of 27 October 1985: a new rupture model from aftershock relocation, focal mechanisms, and stress tensors. *J Seismolog* 17(2):207–222. <https://doi.org/10.1007/s10950-012-9320-9>
- Ousadou F, Dorbath L, Ayadi A, Dorbath C, Gharbi S (2014) Stress field variations along the Maghreb region derived from inversion of major seismic crisis fault plane solutions. *Tectonophysics* 632(2014):261–280. <https://doi.org/10.1016/j.tecto.2014.06.017>

- Ouyed M, Meghraoui M, Cisternas A, Deschamps A, Dorel J, Frechet J, Gaulon R, Hatzfeld D, Philip H (1981) Seismotectonics of the El Asnam earthquake. *Nature* 292(5818):26–31
- Ouyed M, Yielding G, Hatzfeld D, King GCP (1983) An aftershock study of the El Asnam (Algeria) earthquake of 1980. *Geophys J Int* 73(3):605–639
- Philip H, Meghraoui M (1983) Structural analysis and interpretation of the surface deformations of the El Asnam earthquake of October 10, 1980. *Tectonics* 2(1):17–49. <https://doi.org/10.1029/tc002i001.P00017>
- Rothé, JP (1950) Les séismes de Kherrata et la sismicité de l'Algérie, Bulletin du Service de la Carte Géologique de l'Algérie, 4e série Géophysique, 3, Mende, France, 40 pp
- Rothé JP (1955) Le tremblement de terre d'Orléansville et la sismicité de l'Algérie. *Nature (Paris)* 3237:1–9
- Rothé JP, Lepervier C, Truillet R (1977) Les déformations liées au séisme de 1954 d'El Asnam (ex. Orléansville-Algérie). *Bull Soc Geol Fr XIX(3):641–644*
- Roussel J (1973) Les zones actives et la fréquence des séismes en Algérie (1716–1970). *Bull Soc Hist Nat Afr Nord Alger* 64(3 and 4):211
- Santos R., Caldeira B, Bezzeghoud M, Borges JF (2014) The rupture process and location of the 2003 Zemmouri–Boumerdes earthquake (Mw 6.8) inferred from seismic and geodetic data. *Pure Appl Geophys* 172(9):2421–2434
- Santos R, Caldeira B, Bezzeghoud M, Borges JF (2015) The rupture process and location of the 2003 Zemmouri–Boumerdes earthquake (Mw 6.8) inferred from seismic and geodetic data. *Pure Appl Geophys* 172(9):2421–2434. Published online: 23 Nov 2014. <http://dx.doi.org/10.1007/s00024-014-0978-5>
- Shirokova EJ (1967) General features in the orientation of principal stresses in earthquake foci in the Mediterranean Asian seismic belt. *Izv Earth Phys* 1:12–22
- Soumaya A, Ben Ayed N, Delvaux D, Ghanmi M (2015) Spatial variation of present-day stress field and tectonic regime in Tunisia and surroundings from formal inversion of focal mechanisms: geodynamic implications for central Mediterranean. *Tectonics* 33. <https://doi.org/10.1002/2015tc003895>
- Stich D, Ammon CJ, Morales J (2003) Moment tensor solutions for small and moderate earthquakes in the Ibero-Maghreb region. *Geophys Res Lett* 108(B3):2148, ESE 7-1-7-20
- Thio HK, Song X, Saikia CK, Helberger DV, Woods BB (1999) Seismic source and structures estimation in the western Mediterranean using a sparse broadband network. *J Geophys Res* 104(B1):845–861
- Thomas G (1985) Géodynamique d'un bassin intramontagneux : Le bassin du bas Chelif occidental (Algérie) durant le Mio-Plio-Quaternaire. Thèse ès Sciences, Univ. de Pau, p 594
- Van der Woerd J, Dorbath C, Ousadou F, Dorbath L, Delouis B, Jacques E, Tapponnier P, Hahou Y, Menzhi M, Frogneux M, Haessler H (2014) The Al Hoceima Mw 6.4 earthquake of 24 February 2004 and its aftershocks sequence. *J Geodyn* 77:89–109. <https://doi.org/10.1016/j.jog.2013.12.004>
- Wessel P, Smith WHF (1991) Free software helps map and display data. *EOS Trans AGU* 72:441
- Yelles-Chaouche AK, Djellit H, Beldjoudi H, Bezzeghoud M, Buforn E (2004) The Ain Temouchent (Algeria) earthquake of December 22nd, 1999. *Pure Appl Geophys* 161(3): 607–621
- Yielding G, Jackson JA, King GCP, Sinval H, Vita-Finzi C, Wood RM (1981) Relations between surface deformation, fault geometry, seismicity, and rupture characteristics during the El Asnam (Algeria) earthquake of 10 October 1980. *Earth Planet Sci Lett* 56:287–304
- Yielding G, Ouyed M, King GCP, Hatzfeld D (1989) Active tectonics of the Algerian Atlas mountains—evidence from aftershocks of the 1980 El Asnam earthquake. *Geophys J Int* 99(3): 761–788